

The Effect of Acoustic Reflections on Combustor Noise Measurements

Ronald G. Huff*

NASA Lewis Research Center, Cleveland, Ohio

Pressure fluctuations measured in turbine engine combustors at low engine speed show good agreement with theory. Above idle speed, the turbine chokes and a significant change in the shape of the measured combustor pressure spectrum is observed. A theoretical model of the acoustic pressure generated in the combustor due to the turbulence/flame front interaction did not account for acoustic waves reflected from the turbine. By retaining this combustion noise source model and adding a reflecting plane at the turbine and combustor inlet, a theoretical model has been developed that reproduces the undulations in the combustor fluctuating pressure spectra. Plots of the theoretical combustor fluctuating pressure spectra are compared to the measured pressure spectra obtained from the CF6-50 turbofan engine over a range of engine operating speeds. Reasonable agreement exists. It is thus concluded that the simplified combustion noise theory, when modified by a simple turbine reflecting plane, adequately accounts for the changes in measured combustor pressure spectra. The shape of the pressure spectra downstream of the turbine, neglecting noise generated by the turbine itself, will be the combustion noise spectra essentially unchanged, except for the level reduction due to the energy blocked by the turbine.

Nomenclature

A	= cross-sectional flow area, m^2
C	= sonic velocity, m/s
C_p	= specific heat at constant pressure, $J/kg \cdot K$
C_1, C_2	= constants used in complementary function for solving differential equations
F	= functional notation, Eq. (A13)
f	= frequency, Hz
f_0	= fuel/air ratio
g	= acceleration of gravity, m/s^2
H_v	= heating value of fuel, J/kg (cal/kg)
i	$= \sqrt{-1}$
k	= acoustic wavenumber, ω/C_0 , $1/m$
ℓ	= distance between reflecting planes, m
L_b	= burning length (i.e., axial distance measured from flame to point in combustor where chemical reactions ends), m
L_0	= distance to upstream reflecting plane from planar source, m
L_T	= distance to downstream reflecting plane from planar source, m
p_ω	= Fourier-transformed fluctuating pressure, $Pa \cdot s$
R	= reflection factor
T	= mean temperature, K
V	= mean velocity, m/s
\dot{W}	= mean mass flow rate, kg/s
x	= axial distance measured from combustor inlet, positive in direction of flow, m
x_0	= planar source location, measured from upstream reflection plane, m
δ	= time-fluctuating component of density, kg/m^3
η_c	= combustion efficiency
η_p	= acoustic pressure efficiency
ϕ	= phase angle, deg
λ	= fuel mass decay constant, assigned a value of $2\pi/L_b$

ρ	= mean density of fluid, kg/m^3
φ_ω	= Fourier-transformed source terms
ω	= angular frequency, $2\pi f$, rad/s

Subscripts

b	= burning length
L	= left running
R	= right running
T	= total conditions, turbine location
ω	= Fourier-transformed quantity; spectrum
0	= upstream axial location
$1, T$	= axial location downstream of combustion zone
3	= third source term (see Ref. 27)

Introduction

THE reduction of aircraft noise through the use of high-bypass-ratio turbofan engines has revealed another noise source for concern: the core engine. Core engine noise is defined as that produced by the gas generator/turbine/tailpipe combination used to provide shaft power to drive the fan in a turbofan engine. Reference 1 summarizes various combustion noise prediction methods for aircraft engines available before 1974. The methods include both engine and combustor rig predictions.

More recently, it has been recognized that gas generators in Earth-to-orbit propulsion systems create fluctuating pressures that load structures and contribute to the high cycle fatigue failure of critical structures. When prediction of the gas generator fluctuating pressure is required to determine high cycle loading, the methods used to calculate core engine noise can be applied.

Since the publication of Ref. 1, a data bank from various combustion noise experiments has been created by NASA.²⁻⁹ Additionally, a number of engine tests have been performed¹⁰⁻¹⁹ to determine the amount of core engine noise reaching the far-field observer. The acoustic power determined from the data in Refs. 2-9 has been correlated with engine operating parameters in Ref. 20. A number of theoretical investigations is reported in the literature: Ref. 21 sets forth several possible combustion noise source terms to be evaluated; Ref. 22 gives a correlation of data, based on theory, for the acoustic power in a combustor with engine

Presented as Paper 84-2323 at the AIAA/NASA 9th Aeroacoustics Conference, Williamsburg, VA, Oct. 15-17, 1984; received Nov. 14, 1984; revision received July 16, 1985. This paper is declared a work of the U.S. Government and therefore is in the public domain.

*Aerospace Engineer. Member AIAA.

operating parameters; Ref. 23 gives scaling laws for combustion noise radiating from open flames that are based on a theory evolved by using the chemical reactions; Ref. 24 calculates the $1/3$ -octave spectrum for a propane/air open flame; and Ref. 25 points out the need to know the heat release distribution in the combustor before the dynamic design can be performed. References 21-24 have focused attention on combustion noise theory and have presented a fundamental, although at times complex, picture of possible combustion noise mechanisms. Reference 26 has shown that the combustor fluctuating temperatures and pressures are correlated in ducted burners, that the heat release distribution is important, and that the fluctuating volumetric heat release rate needs to be investigated as a source term in combustion generated noise.

In an effort to understand the dominant combustion noise mechanism and to provide a theoretically based prediction that allows insight into the noise-generating parameters in ducted combustors, a simple combustion noise model was derived in Ref. 27. The fluctuating pressure spectrum generated by the interaction of the turbulence with the mean energy gradient in a burner connected to infinite ducts (no reflected waves in either direction) was determined analytically and compared to pressures measured in a CF6-50 turbofan engine combustor. While good agreement existed between the data and the theory, deviations existed above engine idle condition that need to be explained. In the derivation of the acoustic source pressure in Ref. 27, the effect of acoustic waves reflected from both the turbine and combustor inlet planes was neglected.

The objective of the present work is to provide a theoretical solution for the acoustic pressure by a turbulent flame interaction noise source located in a duct between two reflecting planes and to demonstrate that accounting for simple reflections can explain the variation in the narrowband spectral data from the existing theory of Ref. 27.

By understanding the affect of reflections on the fluctuating pressure measured in combustors, one may begin to understand the true combustion noise source mechanism. With the source term and knowledge of the acoustic path transmission characteristics, one may calculate the far-field noise generated by the combustion process. All symbols used herein are defined in the Nomenclature.

Theoretical Model for Combustion Noise with Reflecting Planes

The model for combustion noise considers a one-dimensional, constant-area duct flow (Fig. 1). The flow is composed of a mixture of fuel and air. Turbulence is generated upstream of the flame front by turbulators. The flame front is stabilized aerodynamically at a point just downstream of the turbulators, but does not touch the turbulators. The source region of combustion-related noise starts at the flame front. To simplify the calculations, the flame front is considered to be in a plane perpendicular to the flow direction. The regions upstream and downstream of the source region have constant, although different, properties and are terminated with partial reflecting planes. In engine combustors, the combustion zone temperature varies with the axial distance. In this analysis, the wavenumber is assumed constant in the region downstream of the flame front, thus neglecting any variation in sonic velocity in the combustion zone. The reflecting planes represent the turbine and combustor inlets in a real turbine engine or turbopump.

Infinite Duct Theory

The narrowband fluctuating pressure spectrum measured in the combustor of the CF6-50 engine⁷ has been predicted using a simple source theory in an infinite duct.²⁷ A comparison of the theory with data is shown in Fig. 2 for the engine operating at both low and high thrust. At the idle

condition (Fig. 2a), the theory and data agree very well if the closely spaced minimum value points in the spectrum are ignored. At the 99.8% thrust condition (Fig. 2b), deviation of the measured spectra from that predicted from the infinite duct theory is apparent at frequencies around 300 and 1300 Hz. To account for this deviation, a theoretical analysis including the effects of reflected waves on the measured spectra has been developed. The model, as expected, does not explain the closely spaced minimum value dips in the spectra.

Reflecting Plane Theory

The one-dimensional Fourier-transformed acoustic wave equation with the turbulence flame front noise source term from Ref. 27 is written here as

$$\frac{\partial^2 p_\omega}{\partial x^2} + k^2 p_\omega = -\frac{\dot{W}}{A} \frac{\partial^2}{\partial x^2} \left(\frac{\delta_\omega}{\rho} V \right) \quad (1)$$

For low Mach number flow in the combustor, the right side of Eq. (1) (source forcing function) $\varphi_{3,\omega}$ from Ref. 27 may be written as

$$\varphi_{3,\omega} = -\frac{\dot{W}}{A} \frac{\delta_\omega}{\rho} \frac{V_0 \eta_c H_v f_0 \lambda^2}{C_p T_{T,0}} e^{-\lambda(x-L_0)} \quad (2)$$

The solution of Eq. (1) with source term expression [Eq. (2)] is accomplished using Green's function. First, the duct is divided into two regions: one upstream of a planar source located in the source region and the other downstream of the planar source. Complex reflection factors are defined and the method used for solving the wave equation for a string with source and reflecting points is followed as given in Ref. 28 (pp. 132-138). See the Appendix for the derivation. The equation for the acoustic pressure in the downstream region is from the Appendix [Eqs. (A15) and (A16)],

$$p_{\omega,T} = -i\eta p \frac{\dot{W}}{A} \frac{\delta_\omega}{\rho} \frac{V_0 \eta_c H_v f_0 \lambda^2}{C_p T_{T,0} k_T} (e^{ik_T(t-x)} + R_T e^{-i[k_T(t-x) - \phi_T]}) \times \int_{L_0}^{L_0+L_b} \left[\frac{e^{ik_0 x_0} + R_0 e^{-i(K_0 x_0 - \phi_0)}}{F_0(x_0)} \right] e^{-\lambda(x_0-L_0)} dx_0 \quad (3)$$

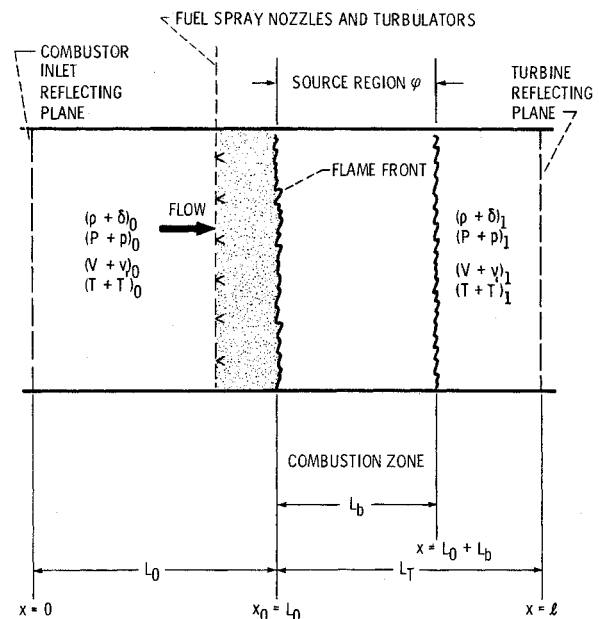


Fig. 1 Combustion noise source model with reflecting planes.

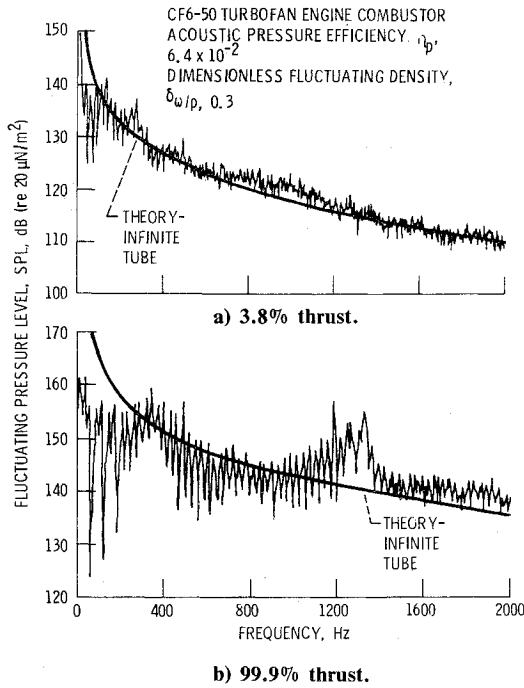


Fig. 2 Comparison of infinite tube theory to measured sound pressure level spectrum.

where the denominator in the integral is

$$F_0(x_0) = \frac{k_0}{k_T} (e^{ik_0 x_0} - R_0 e^{-i(k_0 x_0 - \phi_0)}) \times (e^{ik_T(\ell - x_0)} + R_T e^{-i[k_T(\ell - x_0) - \phi_T]}) + (e^{ik_T(\ell - x_0)} - R_T e^{-i[k_T(\ell - x_0) - \phi_T]}) (e^{ik_0 x_0} + R_0 e^{-i(k_0 x_0 - \phi_0)}) \quad (4)$$

This equation was programmed and integrated numerically over the combustion zone using a computer. The output of the program was the power spectral density of the acoustic pressure.

For comparison purposes the acoustic pressure calculated for the same combustion noise source but in an infinite duct is, from Ref. 27,

$$p_{\omega, R} = \frac{-i}{2} \frac{\dot{W}}{\eta_p A} \frac{\delta_\omega}{\rho} \frac{V_0 \eta_c H_v f_0 \lambda^2 e^{-ikx}}{C_p T_0 k} \int_{L_0}^{L_0 + L_b} e^{-(\lambda - ik)x_0} dx_0 \quad (5)$$

It can be shown that for equal wavenumbers ($k_T = k_0$) and for both reflection factors and phase angles equal zero, Eq. (3) reduces exactly to Eq. (5), as might be expected.

Trends Predicted from Theory

The acoustic pressure as a function of frequency has been calculated using Eqs. (3) and (4). This calculation accounts for reflections from the turbine and the combustor inlet. An acoustic pressure efficiency using infinite tube theory, was calculated in Ref. 27 using fluctuating pressure data measured in a CF6-50 turbofan combustor at the 3.8% thrust level.⁷

The acoustic pressure efficiency η_p as determined in Ref. 27 was 0.045. However, due to the omission of a radical in the equation used to calculate the acoustic pressure efficiency in Ref. 27 and because of terms in the frequency parameter, a corrected value of 0.088 has been used with the present

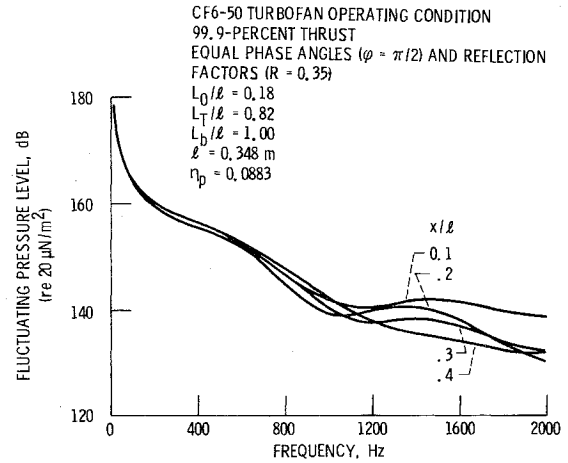


Fig. 3 Effect of measurement location on acoustic pressure spectrum calculated from theory.

theoretical calculations. The narrowband data⁷ used herein were analyzed using a 2 Hz bandwidth filter. All theoretical pressure spectra for comparison purposes have been multiplied by the 2 Hz bandwidth so that they are directly comparable with the as analyzed data reported in Ref. 7.

Measurement Location Effects

The measured fluctuating pressure spectrum reported in Ref. 7 was obtained at the borescope opening in the combustor just downstream of the combustor inlet station. Figure 3 shows the theoretical pressure spectrum at 100% thrust for duct measurement locations $x/\ell = 0.1-0.4$ with the same reflection factor ($R = 0.35$) and phase shift ($\phi = \pi/2$) at both reflecting planes. Little difference exists below 1000 Hz over the range of axial locations shown; however, significant difference exists above 1000 Hz.

Reflection Factor Effect

The magnitude of the reflection factor has a large effect on the spectral shape, as shown in Fig. 4 for the CF6-50 combustor operating at 100% thrust. Figure 4a presents the theoretical narrowband pressure spectrum at $x/\ell = 0.2$ for equal reflection factors of $R = 0.0-0.8$ and a phase angle, $\phi = \pi/2$ rad. Large changes of the spectral shape are noted with changes of R in this range. A string supported between flexible supports and driven sinusoidally behaves in a similar manner.²⁸ From Ref. 28, the solution for the string amplitude function has in the denominator a sine function. The zeros of the sine function yield division by zero, thus giving large string amplitudes or resonant frequencies. For the combustor with reflections the term $F_0(x_0)$ in Eq. (3), under proper conditions approach zero and yields pressure maximums at frequencies of approximately 400 and 1500 Hz. Subsequently, it is shown that these maximums exist in measured spectra and therefore are real. For complete reflection (Fig. 4b), $R_T = R_0 = 1$, the fundamental resonant frequency calculated from $f = C/4\ell$ for the upstream and downstream sonic velocities are on the order of 386 and 529 Hz, respectively, where the values are calculated by treating the combustor as if it were entirely cold or entirely hot, respectively. Within this range of frequencies, several peaks occur in the spectra.

This band of multiple peaks is due to the sources being distributed over the burning length L_b . Mathematically, this is expressed by Eq. (3) where the contribution of the source region to the downstream running wave is obtained by integrating over the burning length L_b . From the physical point of view, one may think of the combustion zone as consisting of a large number of sources. Each source sends a wave to the reflecting surface. The distance to the reflecting

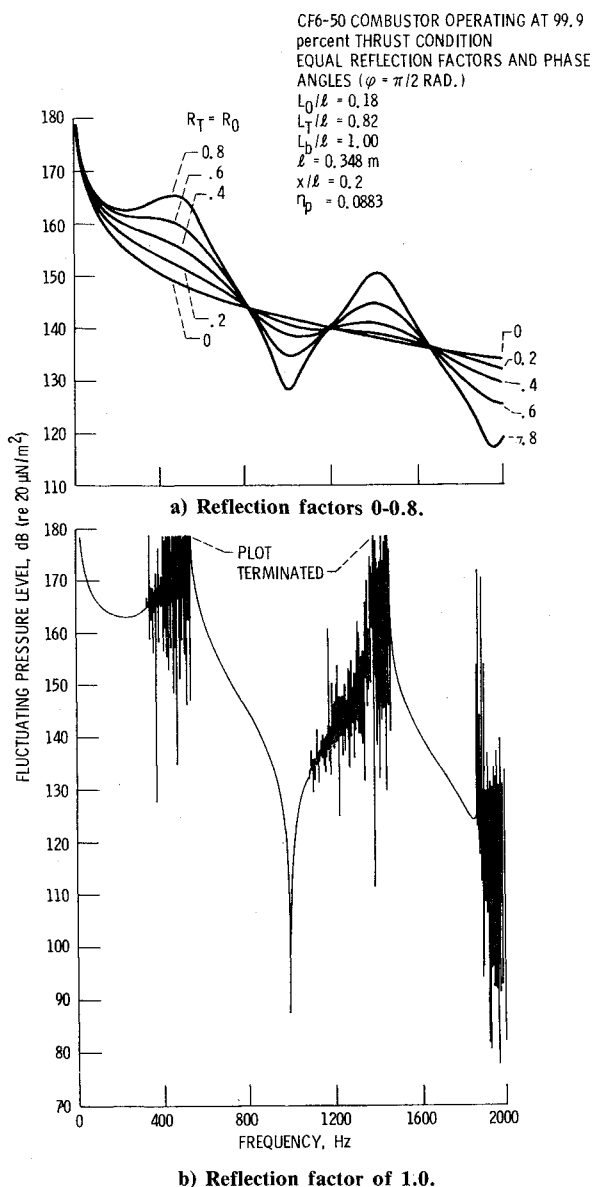


Fig. 4 Theoretical effect of reflection factor magnitude on spectral shape.

plane determines the wavelength and, therefore, frequency at which the reflected and source wave will add together, thus resulting in the resonant condition. Since each source is located at varying distances from the reflecting plane, the resonant wavelengths or frequencies will also vary over some frequency range depending on the burning length. Of course, multiple resonant frequencies bands exist above the fundamental frequency and are shown in the range of 1500 and 2000 Hz in Fig. 4b. As will be shown later, the lower values of the reflection factor appear to be more representative of the data.

Variation of the phase angle associated with the reflection factor, as shown in Fig. 5, has a significant effect on the narrowband spectral shape. Figure 5 presents the theoretical pressure spectrum at the CF6-50 engine 100% thrust condition. The reflection factors are equal with magnitude $R_T = R_0 = 0.35$ and equal but varying phase angles. The variation of the phase angle, $\phi = 0-2\pi$ rad, causes large changes in the spectral shape. All spectra are double humped in the frequency range shown. It appears that more exact knowledge of the phase angle is required if one expects to predict accurately the effect of reflections on combustion-generated noise spectra as obtained from combustor pressure measurements.

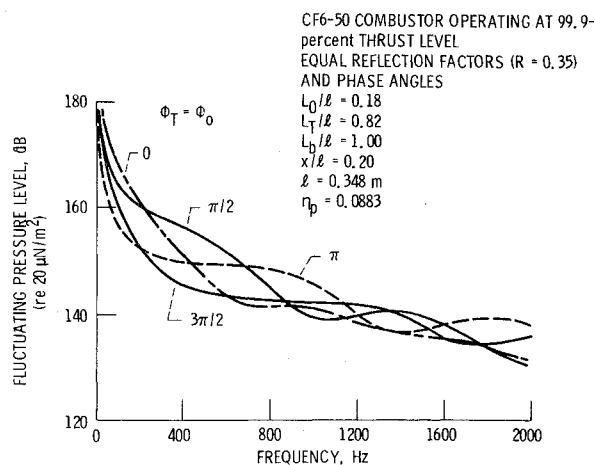


Fig. 5 Theoretical effect of phase angle on spectral shape.

Comparison of Combustor Data with Theory

The narrowband fluctuating pressure spectra from Ref. 7 are shown in Fig. 6 along with the spectra predicted by the present theory. A range of operating conditions from 99.9 to 3.8% of design thrust are shown in Figs. 6a-6d, respectively. As discussed in Ref. 8, the measured spectra above idle setting are bilobed with maximums occurring in frequency regions of 350 and 1100-1300 Hz. The theoretical spectra were calculated for $R_T = R_0 = 0.35$ and $\phi = \pi/2$ and are shown in Fig. 6 by the solid lines. Also shown in Fig. 6 are the calculated spectra for reflection factor equal zero (dashed line). Reference 29 indicates that reflection factors on the order of 0.4 might be expected from turbines.

The theory predicts two humps in the spectra, one centered in the frequency range 200-700 Hz and the other centered in 1000-1600 Hz. The predicted humps, above idle condition, appear to occur at a higher frequency than the humps in the data by 100-200 Hz. Comparisons of the theoretical hump center frequency with increasing engine speed above idle shows that it is predicted to increase with speed. The experimental data also show an increasing hump center frequency with increasing engine speed. The shape of the theoretical spectra and data also show similar trends with frequency. It has been shown that reflection factor phase angles and, at the higher frequencies, the measurement location have significant effect on the spectral shape. Even though the real phase angles and measurement location are not known precisely, it appears that the agreement between theory and experiment is adequate. Taking into account the stated uncertainties, the conclusion is drawn that the deviation of the spectral data above idle conditions from the simple source noise given in Ref. 27 may be attributed to reflections from the turbine and combustor inlet.

At idle condition (Fig. 6d), the theoretical pressure spectrum with reflection factors of zero (see dashed line Fig. 6d) agree with the experimental data. The data do not show a distinct peak in the spectrum where it might be expected if reflections were significant. Reference 29 indicates that the turbine reflection should decrease with turbine pressure ratio. Hence, at the 3.8% thrust level, the turbine reflection factor should approach zero. Judging from the lack of humps in the spectra at the 3.8% thrust level, it appears that little or no reflection exists in the combustor at idle speed and, indeed, the turbine reflection factor is zero. As has been shown in Ref. 27, the infinite tube theory predicts the narrowband spectrum in the CF6-50 combustor very well at the idle condition.

Comments

The present analysis neglects the effects on the acoustic pressure measured between the reflecting planes of both area

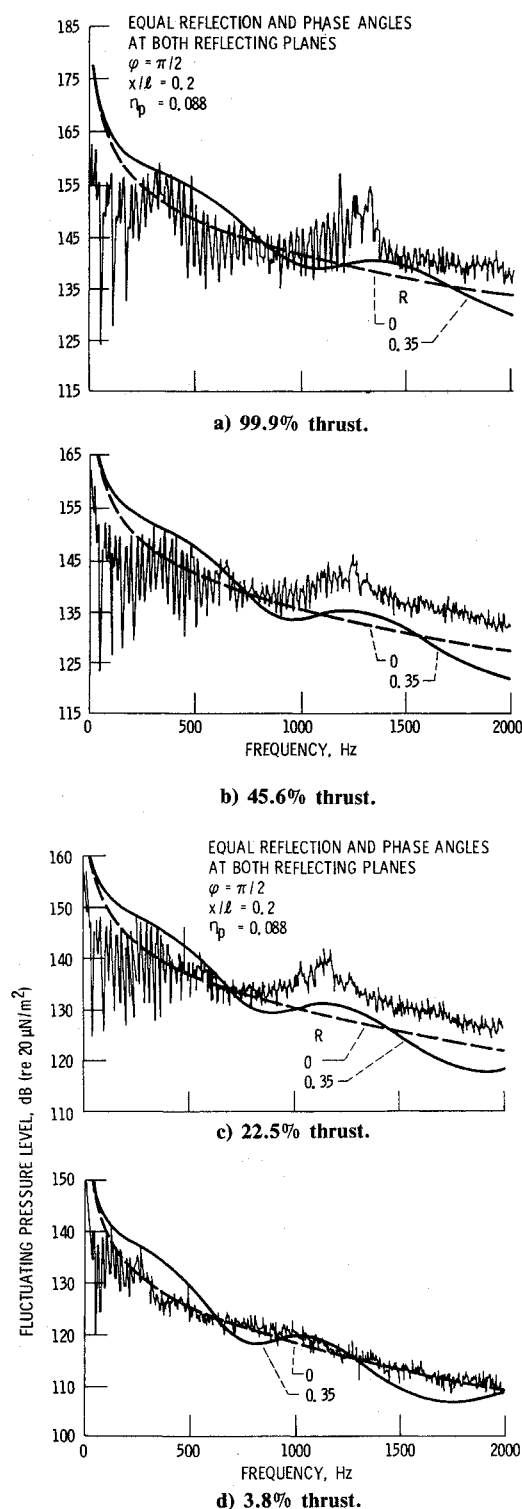


Fig. 6 Comparison of CF6-50 turbofan engine combustor pressure spectra with theoretically predicted values.

variation between reflecting planes and acoustic wavenumber variation within the combustion zone. The analysis in Refs. 25 and 26 includes these effects. However, the present analysis does include the effect of a distributed source. Certain conclusions may still be drawn from the present analysis that appear to explain some of the variations in the spectra from the simple combustion noise source derived in Ref. 27.

It has been shown that reflections from the turbine and combustor inlets are the probable cause for the deviation of the combustor fluctuating pressure spectra from the smooth curve given by the source spectrum. Since the strongest

reflected wave interference with the source can exist only between the reflecting planes, one may conclude that the source wave itself will dominate and essentially be transmitted through the reflecting planes without spectral shape modification. Of course, the magnitude of the source wave will be decreased but the frequency dependence should remain the same. For this reason, one may expect that the acoustic pressure measured external to an engine in the far field will have the very low frequency-dominated spectrum of the combustion noise source as reported in Ref. 27. Cross correlations between combustor and far-field microphones verify this conclusion.⁸

Conclusions

A theoretical investigation of the effect on combustion chamber fluctuating pressures of reflecting planes at the combustor and turbine inlet locations has been performed. The pressure spectrum has been calculated and compared to existing data from a CF6-50 turbofan engine combustor and found to be in substantial agreement. The following conclusions have been drawn from the theory and comparisons of the theory with data:

- 1) At idle engine speed, no reflection from the turbine or combustor inlet occur and the infinite theory applies and yields excellent agreement with the data.
- 2) Above engine idle conditions, reflections from the turbine and combustor inlets occur and reasonable agreement between theory and narrowband combustor pressure spectra has been found using a reflection factor on the order of 0.35 and a phase angle of $\pi/2$ rad.
- 3) Measured spectrum shape is independent of the measurement location at low frequencies, but not at the high frequencies.

Appendix: Solution of the One-Dimensional, Fourier-Transformed Acoustic Wave Equation with Combustion Noise Source Term and Two Reflecting Planes

The acoustic wave equation governing the acoustic pressure generated and measured in a one-dimensional duct with reflecting planes representing the combustor and turbine inlets is, from Ref. 27,

$$\frac{\partial^2 p_\omega}{\partial x^2} + k^2 p_\omega = -\varphi_{3,\omega} \quad (A1)$$

where the source term $\varphi_{3,\omega}$ is given in Ref. 27 as

$$\varphi_{3,\omega} = -\frac{\dot{W}}{A} \frac{\delta_\omega}{\rho} \frac{V_0 \eta_c \eta_p H_v f_0 \lambda^2}{C_p T_{T,0}} e^{-\lambda(x-L_0)} \quad (A2)$$

The homogeneous equation obtained by setting $\varphi_{3,\omega}$ to zero is

$$\frac{\partial^2 p_\omega}{\partial x^2} + k^2 p_\omega = 0 \quad (A3)$$

The solution of Eq. (A3) is

$$p_{\omega,0} = C_1 e^{ikx} + C_2 e^{-ikx} \quad (A4)$$

Resultant wave pressure = left running wave pressure + right running wave pressure

A planar source is assumed to exist in the combustion zone. The regions between the planar source and combustor inlet and the planar source and turbine inlet have different temperatures and, hence, different sonic velocities and fluid properties. At the combustor inlet reflecting plane ($x=0$), the reflection factor, a complex number defined as the com-

plex ratio of the reflected to the incident acoustic pressures, is given by

$$p_{\omega,R}/p_{\omega,L} \equiv R_0 e^{i\phi_0} \quad (A5)$$

and the turbine reflecting plane ($x = \ell$),

$$p_{\omega,L}/p_{\omega,R} \equiv R_T e^{i\phi_T} \quad (A6)$$

The magnitude and phase of both reflection factors are assumed to be constant and known quantities.

The two regions are treated separately until later in the derivation. In the region upstream of the planar source Eq. (A4) may be written in terms of the combustor inlet reflection factor as

$$p_{\omega,0} = C_1 (e^{ik_0 x} + R_0 e^{-i(k_0 x - \phi_0)}), \quad 0 < x < x_0 < \ell \quad (A7)$$

In the region downstream of the planar source, the acoustic pressure is, again written in terms of the turbine reflection factor,

$$p_{\omega,T} = C_2 (R_T e^{-i[k_T(\ell-x) - \phi_T]} + e^{ik_T(\ell-x)}), \quad 0 < x_0 \leq x < \ell \quad (A8)$$

The method used in Ref. 28 for solving the harmonically driven string with reflections is now applied to find the solution of the acoustic wave equation used herein. Equations (A7) and (A8) have two unknown constants, C_1 and C_2 . Therefore, two bits of information are required to solve for these constants. The first requirement is that the pressures across the planar source are continuous, i.e., the pressures at the source are equal for both regions. Equating Eqs. (A7) and (A8) at the source location, $x = x_0$ yields

$$C_1 (e^{ik_0 x_0} + R_0 e^{-i(k_0 x_0 - \phi_0)}) - C_2 (R_T e^{-i[k_T(\ell-x_0) - \phi_T]} + e^{ik_T(\ell-x_0)}) = 0 \quad (A9)$$

From Ref. 28, the difference in the slopes at the planar source is -1 . Taking the derivative with respect to x of Eqs. (A7) and (A8) and equating the differences of the slopes to -1 yields the second expression in terms of C_1 and C_2 as

$$C_1 i k_0 (e^{ik_0 x_0} - R_0 e^{-i(k_0 x_0 - \phi_0)}) + C_2 i k_T (e^{ik_T(\ell-x_0)} - R_T e^{-i[k_T(\ell-x_0) - \phi_T]}) = -1 \quad (A10)$$

Solving Eqs. (A9) and (A10) for C_1 and C_2 and substituting C_1 and C_2 into Eqs. (A7) and (A8), respectively, yields the expression for the acoustic pressure that would be measured in the duct if the duct were forced by the unit impulse function. The resulting acoustic pressures for the two regions are

$$p_{\omega,0} = \left[\frac{i}{k_T} (e^{ik_0 x} + R_0 e^{-i(k_0 x - \phi_0)}) \times (e^{ik_T(\ell-x_0)} + R_T e^{-i[k_T(\ell-x_0) - \phi_T]}) \right] / F_0(x_0), \quad 0 < x < x_0 < \ell \quad (A11)$$

and

$$p_{\omega,T} = \left[\frac{i}{k_T} (e^{ik_T(\ell-x)} + R_T e^{-i[k_T(\ell-x) - \phi_T]}) \times (e^{ik_0 x_0} + R_0 e^{-i(k_0 x_0 - \phi_0)}) \right] / F_0(x_0), \quad 0 < x_0 < x < \ell \quad (A12)$$

where the denominator is a function of the point source location and is given by

$$F_0(x_0) = \frac{k_0}{k_T} (e^{ik_0 x_0} - R_0 e^{-i(k_0 x_0 - \phi_0)}) \times (e^{ik_T(\ell-x_0)} + R_T e^{-i[k_T(\ell-x_0) - \phi_T]}) + (e^{ik_T(\ell-x_0)} - R_T e^{-i[k_T(\ell-x_0) - \phi_T]}) \times (e^{ik_0 x_0} + R_0 e^{-i(k_0 x_0 - \phi_0)}) \quad (A13)$$

Having the solutions, in their respective regions, for the acoustic pressure as a response to the unit impulse function, the acoustic pressure in the duct as a response to the distributed source in the combustion region can be found by integrating the product of the source $\varphi_{3,\omega}$ and the pressure response to the unit impulse over the combustion region as discussed in Ref. 28. In equation form, the pressure in the upstream region is

$$p_{\omega,0} = \frac{i}{k_T} (e^{ik_0 x} + R_0 e^{-i(k_0 x - \phi_0)}) \times \int_{x_0=L_0}^{x_0=L_0+L_b} \left(\frac{e^{ik_T(\ell-x_0)} + R_T e^{-i[k_T(\ell-x_0) - \phi_T]}}{F_0(x_0)} \right) \cdot \varphi_{3,\omega}(x_0) dx_0, \quad 0 < x < x_0 < \ell \quad (A14)$$

and in the downstream region,

$$p_{\omega,T} = \frac{i}{k_T} (e^{ik_T(\ell-x)} + R_T e^{-i[k_T(\ell-x) - \phi_T]}) \times \int_{x_0=L_0}^{x_0=L_0+L_b} \left[\frac{e^{ik_0 x_0} + R_0 e^{-i(k_0 x_0 - \phi_0)}}{F_0(x_0)} \right] \cdot \varphi_{3,\omega}(x_0) dx_0, \quad 0 < x_0 < x < \ell \quad (A15)$$

where $F_0(x_0)$ is given by Eq. (A13) and the source term from Ref. 27 is given by

$$\varphi_{3,\omega} = -\frac{\dot{W}}{A} \frac{\delta_\omega}{\rho} \frac{V_0 \eta_p \eta_c H_v f_0 \lambda^2}{C_p T \tau_0} e^{-\lambda(x_0 - L_0)} \quad (A16)$$

The integration is performed by converting from the complex polar form to the complex rectangular form, integrating the real and imaginary parts separately, and then converting the results of the integration back to polar form. Numerical integration was used in the present work. The pressure calculated using Eqs. (A15) and (A16) is the theoretical acoustic pressure in the duct for the region downstream of the planar source. It was used in making the theoretical acoustic pressure predictions reported herein, since the data used for comparison was taken from a sensor located downstream of the expected flame front location.

References

- Huff, R. G., Clark, B. J., and Dorsch, R. G., "Interim Prediction Method for Low Frequency Core Engine Noise," NASA TM X-71627, 1974.
- Emmerling, J. J., "Experimental Clean Combustor Program; Noise Measurement Addendum, Phase I," General Electric Co., Cincinnati, OH, Rept. GE75AEG315, July 1975 (also NASA CR-134853).
- Sofrin, T. G. and Ross D. A., "Noise Addendum, Experimental Clean Combustor Program, Phase I," Pratt & Whitney Aircraft, East Hartford, CT, Rept. PWA-5252, Oct. 1975 (also NASA CR-134820).
- Emmerling, J. J. and Bekofske, K. L., "Experimental Clean Combustor Program; Noise Measurement Addendum, Phase II," General Electric Co., Cincinnati, OH, Rept. R75AEG147-13-ADD, Jan. 1976 (also NASA CR-135045).

⁵Sofrin, T. G. and Riloff, N. Jr., "Experimental Clean Combustor Program: Noise Study," Pratt & Whitney Aircraft, East Hartford, CT, Rept. PWA-5458, Sept. 1976 (also NASA CR-135106).

⁶Doyle, V. L., "Experimental Clean Combustor Program, Phase III: Noise Measurement Addendum," General Electric Co., Cincinnati, OH, Rept. R78AEG319, Dec. 1978 (also NASA CR-159458).

⁷Doyle, V. L., "Core Noise Investigation of the CF6-50 Turbofan Engine," General Electric Co., Cincinnati, OH, Rept. R79AEG247, Jan. 1980 (also NASA CR-159598).

⁸Doyle, V. L. and Moore, M. T., "Core Noise Investigation of the CF6-50 Turbofan Engine, Final Report," General Electric Co., Cincinnati, OH, Rept. R79AEG395, Jan. 1980 (also NASA CR-159749).

⁹Wilson, C.A. "YF102 In-Duct Combustor Noise Measurement," Vols. I, II and III, AVCO Lycoming Div., Stratford, CT, Rept. LYC-77-56-VOL-1, VOL-2-VOL-3, Nov. 1977 (also NASA CR-135404-VOL-1, VOL-2, VOL-3).

¹⁰Woodward, R. P. and Minner, G. L., "Low-Frequency Rear Quadrant Noise of a Turbojet Engine with Exhaust Duct Muffling," NASA TM X-2718, 1973.

¹¹Burdsall, E. A., Brochu, F. P., and Scaramella, V. M., "Results of Acoustic Testing of the JT8D-109 Refan Engines," Pratt & Whitney Aircraft, East Hartford, CT, Rept. PWA-5298, Nov. 1975 (also NASA CR-134875).

¹²Mathews, D. C. and Peracchio, A. A., "Progress in Core Engine and Turbine Noise Technology," AIAA Paper 74-948, Aug. 1974.

¹³Karchmer, A. M. and Reshotko, M., "Core Noise Source Diagnostics on a Turbofan Engine Using Correlation and Coherence Techniques," NASA TM X-73535, 1976.

¹⁴Reshotko, M., Karchmer, A., Penko, P. F., and McArdle, J. G., "Core Noise Measurements on a YF-102 Turbofan Engine," AIAA Paper 77-21, Jan. 1977.

¹⁵Karchmer, A. M., Reshotko, M., and Montegani, F. G., "Measurement of Far Field Combustion Noise from a Turbofan Engine Using Coherence Functions," NASA TM-73748, 1977.

¹⁶Reshotko, M. and Karchmer, A., "Combustor Fluctuating Pressure Measurements in Engine and in a Component Test Facility: A Preliminary Comparison," NASA TM-73845, 1977.

¹⁷Bilwakesh, K. R., et al., "Core Engine Noise Control Program, Vols. I, II, and III," General Electric, Cincinnati, OH, FAA-RD-74-125-VOL-1, VOL-2, VOL-3, (Vol. I, AD-A013128/4; Vol. II, AD-A013129/2; Vol. III, AD-A013131/8), Aug. 1974.

¹⁸Matta, R. K., Sandusky, G. T., and Doyle, V. L., "GE Core Engine Noise Investigation, Low Emission Engines," General Electric Co., Cincinnati, OH, Rept. FAA-RD-77-4, 1977 (AD-A048590), Feb. 1977.

¹⁹Mathews, D. C., Rekos, N. F. Jr., and Nagel, R. T., "Combustion Noise Investigation Predicting Direct and Indirect Noise from Aircraft Engines," Pratt & Whitney Aircraft Group, East Hartford, CT, Rept. PWA-5478 (AD-A038154/1), Feb. 1977.

²⁰von Glahn, U. H., "Correlation of Combustor Acoustic Power Levels Inferred from Internal Fluctuating Pressure Measurements," NASA TM-78986, 1978.

²¹Chiu, H. H. and Summerfield, M., "Theory of Combustion Noise," Princeton University, Princeton, N.J. AMS-1136, (AD-AA001108), July 1973.

²²Muthukrishnan, M., Strahle, W. C., and Handley, J. C., "The Effect of Flame Holders on Combustion Generated Noise," AIAA Paper 76-39, Jan. 1976.

²³Hassan, H. A., "Scaling of Combustion-Generated Noise," *Journal of Fluid Mechanics*, Vol. 66, Nov. 25, 1974, pp. 445-453.

²⁴Stephenson, J. and Hassan, H. A., "The Spectrum of Combustion-Generated Noise," *Journal of Sound and Vibration*, Vol. 53, July 22, 1977, pp. 283-288.

²⁵Mahan, J. R. and Kaspar, J. M., "Influence of Heat Release Distribution on the Acoustic Response of Long Burners," ASME Paper 79-DET-31, Sept. 1979.

²⁶Miles, J. H. and Krejsa, E. A., "A Theoretical Model for the Cross Spectra Between Pressure and Temperature Downstream of a Combustor," *Journal of the Acoustical Society of America*, Sup. 1, Vol. 75, May 1984 (also NASA TM-83671).

²⁷Huff, R. G., "Simplified Combustion Noise Theory Yielding a Prediction of Fluctuating Pressure Level," NASA TP-2237, 1984.

²⁸Morse, P. M. and Ingard, K. Uno, *Theoretical Acoustics*, McGraw-Hill Book Co., New York, 1968, pp. 135-138.

²⁹Matta, R. K. and Mani, R., "Theory of Low Frequency Noise Transmission Through Turbines," General Electric Co., Cincinnati, OH, Rept. R77AEG570, March 1979 (also NASA CR-159457).